

Brazing as a means of sealing ceramic membranes for use in advanced coal gasification processes

K.S. Weil*, J.S. Hardy, J.P. Rice, J.Y. Kim

Pacific Northwest National Laboratory, 902 Battelle Blvd, P.O. Box 999, Richland, WA 99352, USA

Received 11 October 2004; received in revised form 4 May 2005; accepted 15 July 2005
Available online 15 September 2005

Abstract

Coal is potentially a very inexpensive source of clean hydrogen fuel for use in fuel cells, turbines, and various process applications. To realize its potential however, efficient low-cost gas separation systems are needed to provide high purity oxygen that will enhance the coal gasification reaction and to extract hydrogen from the resulting gas product stream. Several types of inorganic membranes are being developed for hydrogen or oxygen separation, including porous alumina, transition metal oxide perovskites, and zirconia. Because they form the heart of the working device, numerous advances have been made in the fabrication and performance of these membrane materials. However, less emphasis has been placed on the materials that will be used in the balance of the device; in particular, the seals that bond the functional ceramic to the metallic structural component. In an effort to begin addressing this issue, we have examined ceramic-to-metal brazing as a method of sealing a model set of gas separation component materials: yttria-stabilized zirconia and stainless steel. In comparative high-temperature exposure testing of joints prepared using commercial brazes and a newly conceived braze alloy, the commercial material proved to be unsuitable due to excessive oxidation. On the other hand, the new material not only displayed superior oxidation resistance, but also excellent hermeticity in prototypic membrane testing. © 2005 Elsevier Ltd. All rights reserved.

1. Introduction

In the US, coal-based integrated gasification combined cycle (IGCC) systems are recognized as the power generation platform of the future not only to deliver clean, low-cost, and efficient base-load electric power, but to also co-produce hydrogen and hydrogen-based products [1,2]. In order to realize this goal however, efficient and low-cost membrane-based gas separation systems are needed to provide high purity oxygen that will enhance the coal gasification reaction [3], eliminate NO_x formation [4], and mitigate the generation of greenhouse gases [5] and to extract hydrogen from the resulting gas product stream, which increases further hydrogen formation via the water-gas shift reaction [6] as well as isolates the purified gas for later use as a fuel or chemical commodity [7]. Additionally with the continued development of solid oxide fuel cell (SOFC) power generation systems, there will be a means of eventually improving efficiencies from the

33–35% maximum achieved in conventional coal-fired power plants [8] to beyond 60% [9,10].

Central to both of these nascent high-temperature technologies is an electrochemically active ceramic membrane through which ion transport takes place either under an imposed pressure gradient, as with oxygen and hydrogen separation [11,12], or under a chemical gradient in the case of power generation via SOFCs [13]. Because these processes are dependent on the magnitude of the ionic gradient that develops across the ceramic membrane, which in turn is proportional to the applied pressure or chemical gradient, hermeticity is paramount [14]. Not only must the membrane be dense with no interconnected porosity, but also it must be connected to a heat-resistant support structure via a gas-tight and mechanically robust high-temperature seal. That is, fabrication of a durable ceramic-to-metal seal is a key enabling technology in the development of these types of electrochemical devices and, in fact, has become a critical technical issue in the long-term success of planar SOFC technology [15]. Examples of the types of seals that are envisioned for large-scale gas separators and planar SOFCs are shown in Fig. 1(a) and (b). While glass bonding is potentially a viable method of sealing in these applications and has been employed in a number of short-term demonstrations, there are issues of compatibility with

* Corresponding author. Tel.: +1 509 375 6796; fax: +1 509 375 4448.
E-mail address: scott.weil@pnl.gov (K.S. Weil).

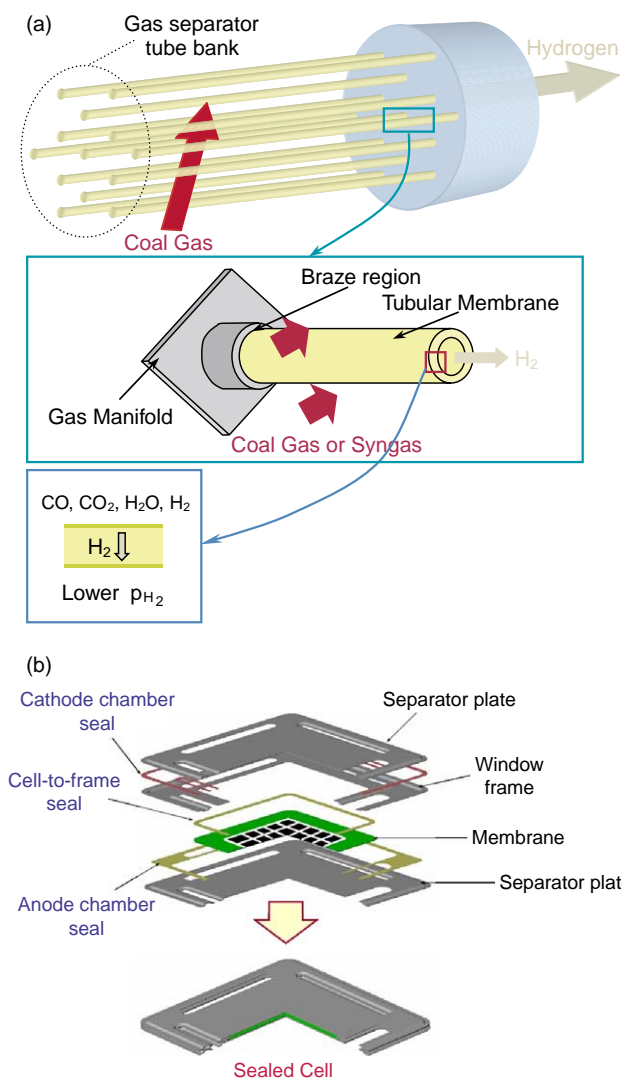


Fig. 1. Schematics of potential coal-gas electrochemical applications where high-temperature sealing is required: (a) a bank of gas separation tubes (either air or hydrogen; coal gas \rightarrow hydrogen is shown) and (b) a planar SOFC cell (one of many in a given stack).

the adjacent substrates [16,17] and problems concerning thermal expansion matching [18] that ultimately affect the longevity and thermal cycling performance of the glass sealed joint.

Alternatively, one of the most reliable and best-understood methods of joining dissimilar materials is by brazing. In this technique, a filler metal whose liquidus is well below that of the materials to be joined is heated to a point at which it becomes molten and fills the gap between the two pieces under capillary action. Upon cooling, a solid and hermetic joint forms. When applied to the bonding of ceramics, a reactive metal such as Ti or Zr is typically added to the base filler metal (thereby forming an active metal braze alloy), which causes reduction of the ceramic substrate during filler melting. This chemically reduced surface is then readily wetted by the remaining braze material [19]. However, before a given braze alloy can be considered for high temperature use (700–800 °C), as envisioned in both gas separation and SOFC applications, its behavior under

prototypical operating conditions must be thoroughly evaluated. In this paper, we summarize the high-temperature (800 °C) results obtained from an extensive series of oxidation tests conducted on joining specimens brazed with two different commercial filler metals [20] and those prepared using alternate approach referred to as air brazing. The latter technique is a unique concept currently under development in our laboratory. As with active metal brazing, air brazing can be used to join ceramic and metal substrates [21]. However unlike active metal brazing, which must be conducted in vacuum or inert gas to avoid oxidation of the filler metal, air brazing takes place directly in air without need of an inert cover gas or the use of surface reactive fluxes [22,23]. This is because the process employs an alloy that consists of a metal oxide dissolved in noble metal filler, i.e. the two materials are mutually soluble when molten. There are several potential filler metal systems that can be considered, including Pt–Nb₂O₃, Ag–CuO, and Ag–V₂O₅ [24]. Here, we discuss our work on a formulation that contains 4 mol% CuO in silver.

2. Experimental methods

Yttria-stabilized zirconia (YSZ, 8% yttria addition; Tosoh Corporation) and thin gauge ferritic stainless steel were selected as the model ionic conducting membrane/structural metal system for this study based on the similarity between their coefficients of thermal expansion (within \sim 8%) over the temperature range of interest, i.e. room temperature to \sim 1000 °C. In joining specimens prepared using the commercial brazes, 12 mil (\sim 300 μ m) thick 430 stainless steel foil (430SS, 18 at.% Cr, $>$ 1 at.% Si, bal. Fe; Allegheny Ludlum corporation) was employed, whereas in the air brazed joints, 2 mil (\sim 50 μ m) thick FeCrAlY foil (22% Cr, 7% Al, 0.1%La+Ce, bal. Fe; Engineered Materials Solutions, Inc.) was used. Because of its excellent oxidation resistance, FeCrAlY was desired for use in all of the joining sample, but was found to be incompatible with the commercial filler metals because of poor wettability on the thin alumina scale that forms during vacuum brazing. To prepare the joining specimens, both metals were metals were cut into washers measuring 44mm in outside diameter with a 15mm diameter concentric hole via electrical discharge machining. The sealing surfaces were left in the as-received rolled condition, but were degreased ultrasonically in acetone for 10 minutes and wiped with methanol prior to use. The YSZ substrates used in the joining specimens were fabricated by tape casting and sintering procedures developed at Pacific Northwest National Laboratory [25]. The final diameter and thickness of the ceramic discs were nominally 18 mm and 200 μ m, respectively.

Two widely used commercial ceramic-to-metal brazing alloys were selected for this study, Gold ABA (3% Ni, 0.6% Ti, balance Au by weight) and Niro ABA (16% Ni, 0.75% Mo, 1.25% V, balance Au by weight). Both were obtained from Wesgo Corporation as 0.15 mm thick sheet. The Ag–CuO air braze composition used in this study, 4 mol% CuO in silver, was chosen based on previously reported YSZ and FeCrAlY wetting and joint strength data [26]. The material was prepared

by ball milling silver powder (99.9%, Alfa Aesar) with an appropriate amount of copper powder (99%, Alfa Aesar) such that when the copper is fully oxidized during air brazing, the target composition would be achieved. A liquid organic binder (B75717, Ferro Corp.) was added to the dry powder mixture in a 1:1 weight ratio to form a paste that could be readily applied to the surfaces of the joining substrates.

Specimens joined using the active metal brazes were prepared by first stacking a YSZ disc on top of a 430SS sample with a $1/2 \text{ cm}^2$ piece of braze foil placed in between, then heating the resulting sandwich under 1×10^{-6} Torr vacuum at $3 \text{ }^\circ\text{C}/\text{min}$ to the brazing temperature recommended by the filler metal manufacturer, holding at this temperature for 1/2 h, and cooling at $3 \text{ }^\circ\text{C}/\text{min}$ to room temperature. A brazing temperature of $1080 \text{ }^\circ\text{C}$ was employed for Au ABA and $1010 \text{ }^\circ\text{C}$ for Nioro ABA. In preparing air brazed samples for oxidation testing, no. 5 braze paste was spread on the faying surfaces of the YSZ and FeCrAlY substrates, which were brought together to form a pre-brazed assembly. Heating was conducted in a muffle furnace using the following schedule: (1) heat in static air at $3 \text{ }^\circ\text{C}/\text{min}$ to $1000 \text{ }^\circ\text{C}$, (2) hold at $1000 \text{ }^\circ\text{C}$ for 1 h and (3) cool to room temperature at $5 \text{ }^\circ\text{C}/\text{min}$. Examples of the components and final specimen used in this study are shown in Fig. 2(a). Exposure testing was conducted in a tube

furnace by slowly heating ($5 \text{ }^\circ\text{C}/\text{min}$) the joining specimens in $20 \text{ cm}^3/\text{min}$ of flowing dry air to $800 \text{ }^\circ\text{C}$ and holding for a given period of time. The composition and microstructure of the oxidized samples were compared against the baseline microstructure of the as-brazed specimen in the unoxidized state using a JEOL JSM-5900LV scanning electron microscope (SEM; JEOL USA) equipped with an Oxford energy dispersive X-ray analysis system (EDX; Oxford Instruments).

As a means of characterizing the hermeticity of the seals, two tests were conducted. In the first, the brazed disk-shaped specimens were pressure tested up to 10 psi. The test was performed by placing the sealed specimen into a pressurization test fixture, schematically shown in Fig. 2(b), and slowly pressurizing the backside of the sample using a digital regulator up to the set point of 10 psi. Once the valve prior to the regulator is closed, approximately 40 ml of compressed gas is isolated between the specimen and the regulator and leaking can be identified by monitoring any decay in pressure. Specific details concerning the design of the test apparatus and the testing procedure have been previously reported in Ref. [18]. Those sealing materials that appeared to yield a hermetic joint based on pressure testing were then subjected to a second, more quantitative test. In this test, one end of a 430 stainless steel tube was brazed to the YSZ side of a miniature anode-supported SOFC cell, which consisted of a porous $500 \text{ }\mu\text{m}$ thick NiO-YSZ anode bonded to a $7 \text{ }\mu\text{m}$ thick dense YSZ electrolyte with a $\sim 20 \text{ }\mu\text{m}$ thick porous lanthanum strontium manganite ($\text{La}_{0.8}\text{Sr}_{0.2}\text{MnO}_3$; LSM) cathode and which measured $\sim 25 \text{ mm}$ in diameter. The hermeticity of the joint was characterized by monitoring the open circuit voltage (OCV) of the cell as a function of time at $750 \text{ }^\circ\text{C}$ as wet hydrogen was passed through the anode chamber and air flowed over the cathode. By comparing the measured OCV with that predicted by the Nernst equation, Eq. (1), for the above operating conditions, any existing leak can be quantified:

$$V_{\text{OC}} = \frac{RT}{4F} \ln \left(\frac{p_{\text{O}_2(\text{c})}}{p_{\text{O}_2(\text{a})}} \right) \quad (1)$$

where V_{OC} is the open circuit voltage, R is the universal gas constant, T is temperature, F is the Faraday constant, and $p_{\text{O}_2(\text{c})}$ and $p_{\text{O}_2(\text{a})}$ are the partial pressures of oxygen on the cathode and anode sides of the cell, respectively.

3. Results

3.1. Gold ABA and Nioro ABA brazed joints

Shown in Fig. 3(a) and (b) are back scattered electron images of the YSZ/Gold ABA/430SS and YSZ/Nioro ABA/430SS joining specimens in the as-brazed condition. As seen in both micrographs, the stainless steel substrate partially dissolves into the filler metal alloy giving rise to three characteristic regions between the two substrates: (1) an interfacial zone between the YSZ and the filler metal, (2) the bulk filler metal region containing an array of iron-rich precipitates, and (3) an interdiffusion zone between the filler

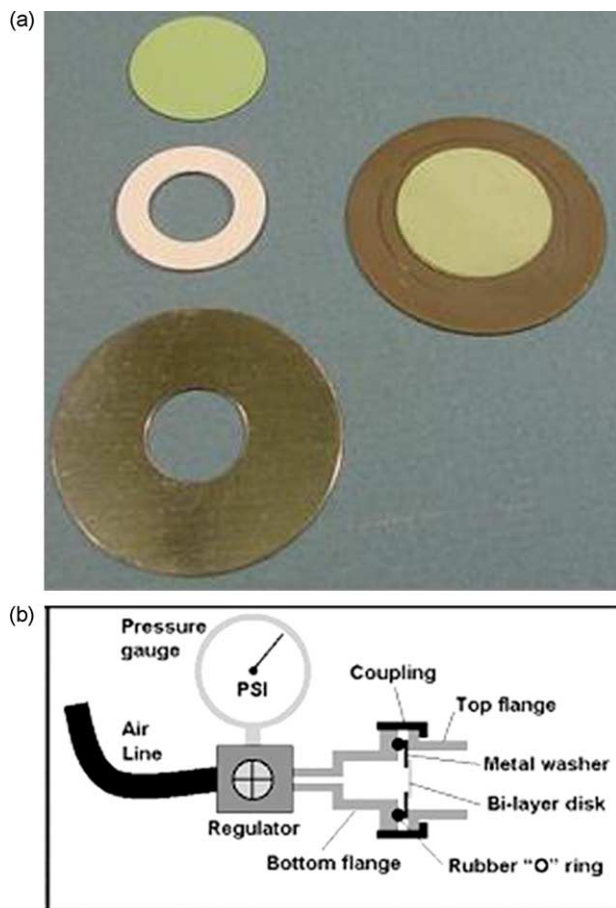


Fig. 2. (a) Components used in preparing specimens for exposure and hermeticity testing. (b) A schematic illustration of the apparatus used in pressurization testing.

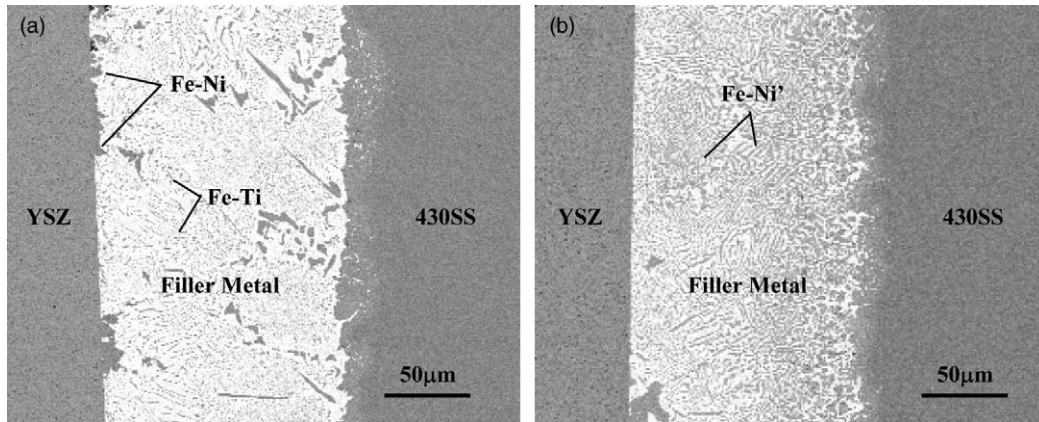


Fig. 3. Cross-sectional SEM micrographs of YSZ/braze/430SS joining samples in the as-brazed condition: (a) Gold ABA and (b) Nioro ABA.

metal and 430SS substrate that contains micron-sized gold-rich precipitates in an iron-based matrix. Due to dissolution and subsequent diffusion into the filler metal during brazing, the 430SS substrate appears to have a significant affect on the chemistry and morphology of the reaction zone. A typical YSZ/active metal braze couple exhibits a distinctive continuous layer of reduced titanium oxide (TiO_x) measuring $\sim 0.5\text{--}1\ \mu\text{m}$ thick along this interface [27]. However, neither joint in Fig. 3 appears to exhibit such a reaction zone. Instead, using EDX we found increased amounts of oxygen, approximately 15–20 at.% in a 1–2 μm thick region adjacent to the YSZ, the concentration of which decays rapidly further into the bulk filler metal. Thus some reduction of the YSZ did occur, allowing for subsequent wetting of this substrate by the 430SS-modified filler metal.

In the Gold ABA specimen, the partial dissolution of the 430SS substrate adds a substantial amount of iron and chromium into the bulk filler metal region during melting. As a result, not only is the gold matrix enriched, but also a series of fine-scale Widmanstätten type iron-titanium precipitates (labeled Fe–Ti; average composition: 54 at.% iron, 23 at.% titanium, 4 at.% nickel, 4 at.% chromium, 12 at.% gold, and 13 at.% oxygen) forms along crystallographically related planes within the matrix. Also found are blocky iron–nickel precipitates (labeled Fe–Ni) along the interface with the YSZ.

Both the iron–nickel precipitates and the matrix contain measurable amounts of chromium, on the order of 7–11 at.%. A similar effect is observed in the Nioro ABA specimen, except that the additional nickel in the original braze leads to the formation of larger, more elongated iron–nickel precipitates that contain significantly less chromium (labeled Fe–Ni'; average composition: 48 at.% iron, 28 at.% nickel, 17 at.% gold, 2 at.% chromium, 1 at.% titanium, and 4 at.% oxygen).

Shown in Fig. 4(a) and (b) are the SEM results obtained on the Gold ABA and Nioro ABA brazed YSZ/430SS joints tested in air at 800 °C for 200 and 50 h, respectively. In the oxidized Gold ABA joining specimen, a continuous oxide layer forms along the ceramic substrate. Measuring $\sim 4\ \mu\text{m}$ in thickness, this layer is composed essentially of Cr_2O_3 , doped with a small amount of iron and nickel. As a high-temperature ionic conductor, YSZ will actively transport oxygen ions across an established chemical gradient; in this case from the air side of the membrane ($p\text{O}_2 \sim 0.2\ \text{atm}$) to the braze side ($p\text{O}_2 \ll 0.2\ \text{atm}$). Even though oxidation internal to the joint takes place, the interfacial chromia layer that forms appears to protect the rest of the braze from a more rapid and intrusive form of oxidation, of the type observed in the oxidized Nioro ABA joint of Fig. 4(b).

The latter specimen shows complete separation along the YSZ/braze interface. The sub-membrane scale that forms,

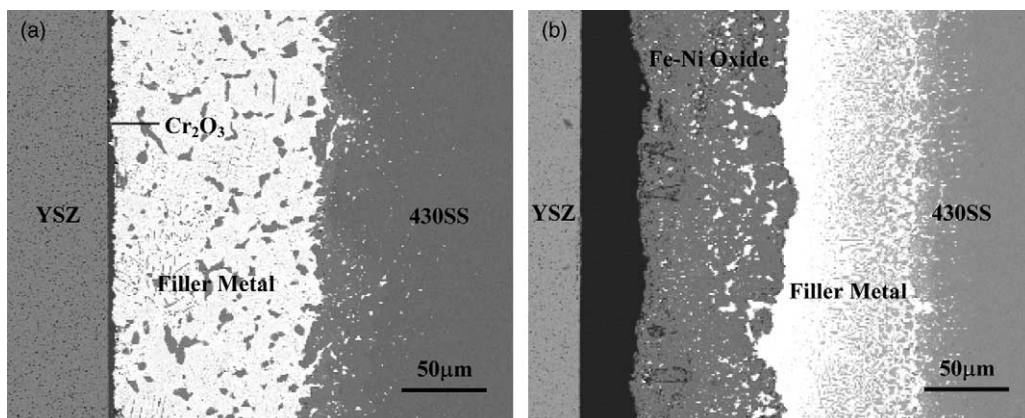


Fig. 4. Cross-sectional SEM micrographs of YSZ/braze/430SS joining samples after oxidation testing in air at 800 °C: (a) Gold ABA, tested for 200 h and (b) Nioro ABA, tested for 50 h.

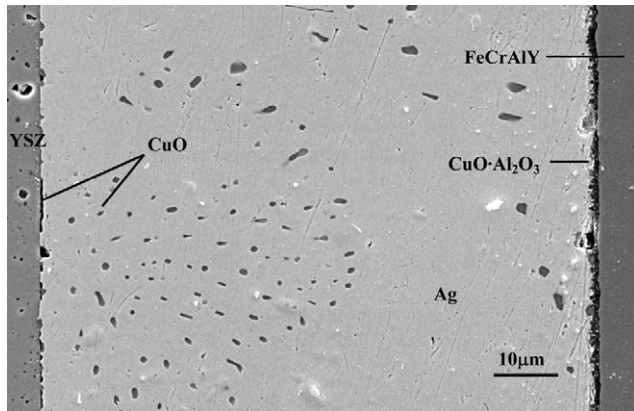


Fig. 5. Cross-sectional SEM micrograph of a YSZ/FeCrAlY joint prepared by air brazing with Ag–4CuO for 1 h at 1050 °C in air.

again due to oxygen transport through the YSZ, is a 50 μm thick oxide layer rich in iron and nickel that exhibits some porosity and a significant amount of internal cracking. This scale layer forms because of availability of nickel and iron and apparent lack of chromium in the precipitates adjacent to the YSZ in the original as-brazed joint. The growth rates of iron- and nickel-based oxide scales are significant greater than that for Cr₂O₃ at these temperatures [28], which accounts for the difference in scale thickness between the Niro ABA and Gold BA specimens. While both the braze filler metals yielded hermetic specimens in the as-joined condition, as measured by zero decay in pressure during subsequent pressurization testing, the as-oxidized specimens displayed no hermeticity. The 50 h Niro ABA brazed specimens leaked immediately, while the 200 h Gold ABA specimens ruptured and leaked during testing.

3.2. Ag–CuO air brazed joints

It is readily apparent that neither the Niro ABA nor the Gold ABA brazes will not work in these high temperature applications. With this in mind, we investigated air brazing as an alternative joining technique. Shown in Fig. 5 is a cross-

sectional micrograph of a YSZ/FeCrAlY joint that was prepared using a 4 mol% CuO in Ag braze composition (Ag–4CuO). At the interface with the YSZ, a nearly continuous layer of silver is found, which is decorated by discrete micron-size islands of CuO attached to the original faying surface. The Ag–CuO phase diagram [29] indicates for this composition that a homogeneous single phase liquid forms at 1050 °C. Upon cooling to the eutectic temperature, solid Ag and CuO nucleate heterogeneously from the eutectic liquid, forming an interspersed morphology of silver and copper oxide along the braze substrate interface. Ideally the resulting solid should consist of a lath-type morphology commonly observed in eutectic alloys [30]. However, the rapid cooling rate employed in air brazing appears to have suppressed the formation of this characteristic microstructure. On the other side of the joint, contiguous to the micron-thin alumina scale on the FeCrAlY component, an interfacial reaction zone is apparent, which contains a thin and patchy layer of CuO and Al₂O₃ in solid solution that is frequently penetrated by fingers of silver and CuO that extend back into the bulk of the braze.

Oxidation of the air brazed joint as a function of time at 800 °C is seen in the two series of micrographs in Figs. 6 (YSZ/filler metal interface) and 7 (filler metal/FeCrAlY interface). It is immediately obvious from these images that neither the bulk matrix of the braze nor the corresponding interfaces change significantly with time at temperature. The YSZ/filler metal interface remains completely stable out to 1000 h of exposure, while the reaction zone between the filler metal and the FeCrAlY exhibits a very minor amount of coarsening in the CuO and mixed oxide particulate over the same time period. Strength measurements of the air brazed YSZ/FeCrAlY joints using the same four-point bend test procedure and specimen configuration reported elsewhere [31] displayed no significant reduction in joint strength attributable to high-temperature air exposure: 78 MPa in the as-brazed condition, 74 MPa after 200 h of exposure in 800 °C air, and 77 MPa after 1000 h of exposure.

Initial pressurization testing indicated no loss in hermeticity in the air brazed specimens from the as-joined condition to the 1000 h as-oxidized condition. Subsequently, OCV testing was

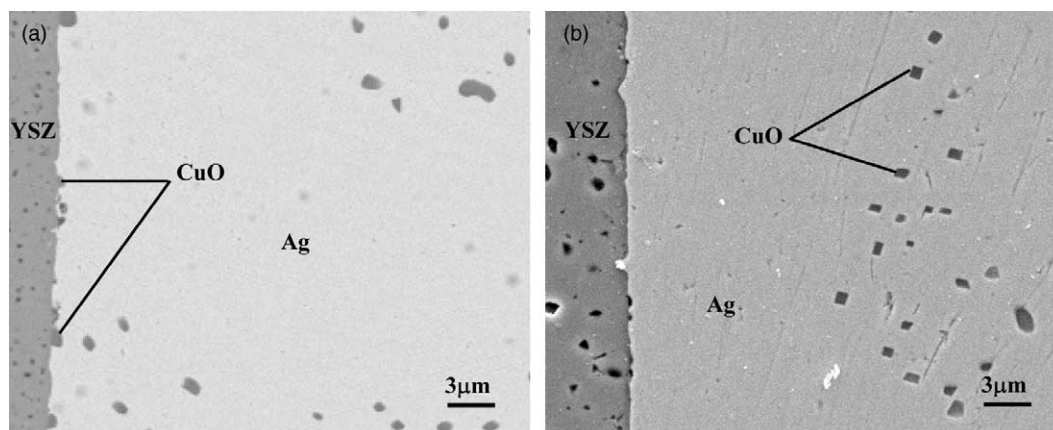


Fig. 6. Cross-sectional SEM micrographs of the YSZ/filler metal region in air brazed joining samples that have undergone testing in 800 °C air for: (a) 200 h and (b) 1000 h.

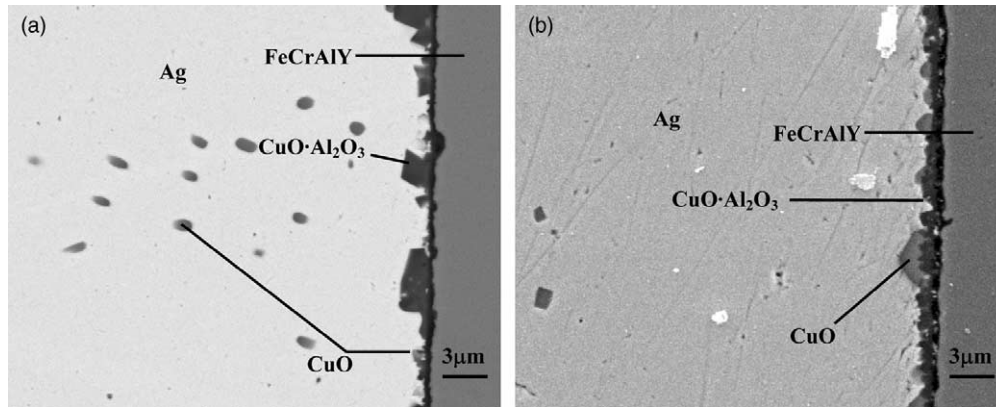


Fig. 7. Cross-sectional SEM micrographs of the filler metal/FeCrAlY region in air brazed joining samples that have undergone testing in 800 °C air for: (a) 200 h and (b) 1000 h.

conducted to determine if leaking could be observed in situ during high-temperature operation. Shown in Fig. 8 are the results from a 250 h test conducted at 750 °C. The OCV is initially 1.084 V and remains essentially constant throughout the test. The OCV predicted from Eq. (1) at 750 °C is 1.085 V and the difference between the two is within experimental error (± 0.05 V) for this measurement technique, suggesting that the air brazed seal is initially hermetic and remains so at temperature out to at least 250 h. Longer-term high-temperature testing is being conducted to determine the potential operational lifetime of the air brazed seal.

Encouraged by these findings, we initiated a demonstration study aimed at incorporating this method of joining into a full-scale SOFC test stack. The first such stack consisted of three 144 mm × 98 mm cells [32]. The Ag–4CuO braze paste was dispensed onto the YSZ side of each cell and the cell was fixtured against a corresponding Crofer-22 APU frame. Brazing was conducted in ambient air at 1050 °C for 15 min, forming a peripheral seal that measured on average ~3 mm wide by ~100 μm thick. The brazed frames were then sealed together using a conventional barium aluminosilicate based glass to prevent shorting between adjacent cells. In a fully brazed stack, an electrical insulator (possibly a coating over the sealing surfaces of the separator plates) would need to be

incorporated into the brazed seals between each repeat unit to avoid shorting. After final assembly and initial start-up, the stack was operated at 750 °C for 120 h on 2 lpm of 48.5% H₂, 48.5% N₂, 3% H₂O fuel gas flow on the anode side and 4 lpm of air flow on the cathode side. Both gases were pre-heated to ~550 °C prior to entering the stack.

While the stack exhibited a steady decline in current output over this period of operation, from an initial value of 253.5–231.7 A at 21% fuel utilization and a control voltage of 0.7 V average per cell, a near theoretical open circuit voltage was realized throughout, 3.23 V on average, implying that the seals remained hermetic during the entire operation. Experience based on in-house single cell testing, combined with the post-test analysis results of the stack suggest that the power degradation observed in this test is attributable to chromia volatilization. SEM analysis of the seals, shown in Fig. 9, indicates that the braze microstructure undergoes little change due to stack operation. Note however that the interface formed between the braze and Crofer differs significantly from that observed in the FeCrAlY specimens, for example in Fig. 5. The interfacial zone is measurably thicker, on the order of 10 μm, displays an undulating morphology, and consists primarily of fingers of silver that infiltrate between discrete precipitates of

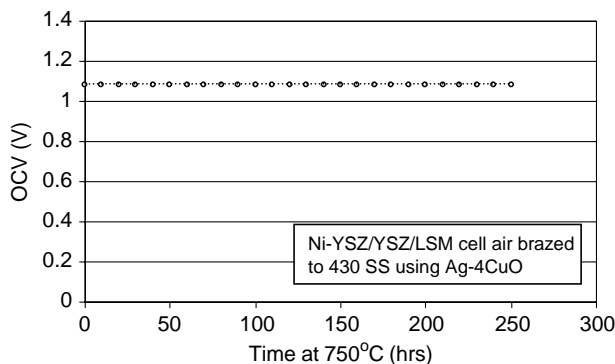


Fig. 8. Open circuit voltage of a nickel-YSZ/YSZ/LSM electrochemical cell air brazed to a stainless steel tube as a function of time at 750 °C. The cathode side of the cell was exposed to air and the anode side to wet hydrogen.

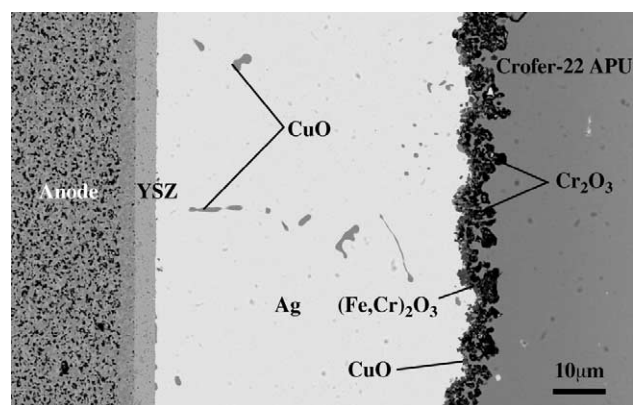


Fig. 9. Cross-sectional SEM micrographs of a brazed joint in a full-scale stack that underwent 120 h of operation at 750 °C. The composition of the braze is 4 mol% CuO in Ag.

copper oxide and two interfacial oxidation products, $(\text{Fe,Cr})_2\text{O}_3$ and Cr_2O_3 . Additional testing on air brazed SOFC seals as well as on those used in hydrogen and oxygen separation tubes is being conducted to determine the high-temperature stability of the this novel sealing material over longer periods of time.

4. Conclusions

Oxidation testing of YSZ/stainless steel joints prepared using two commercial brazes indicated that these materials are unsuitable for high temperature application. Specifically, substantial amounts of iron and chromium are introduced into the filler metal due to partial dissolution of the underlying stainless steel substrate during brazing. Because oxygen ion transport takes place through the YSZ membrane at high temperature, oxidation of these species, as well as the nickel in the original braze alloy, takes place at the YSZ/filler metal interface. In the case of a high nickel content filler metal, such as Niro ABA, oxidation is rapid, forming a non-protective iron–nickel scale that leads to immediate joint failure. However even with a lower nickel containing filler metal such as Gold ABA, sub-membrane oxidation occurs, in this case forming a continuous Cr_2O_3 layer. Although chromia is protective at high temperature, membrane spallation or joint fracture is expected when the scale eventually grows too thick.

Alternatively when the air brazing alloy is employed, little change occurs in the joint upon high-temperature air exposure. This is because joining is conducted directly in air at a temperature higher than that employed in the test or application. In essence, the joint is pre-oxidized such that very little additional oxidation occurs during subsequent high temperature use. In addition to being oxidation resistant, the braze also proved to be hermetic, at least up to 250 h under dilute fuel gas, as demonstrated in initial electrochemical testing of an SOFC stack that contained air brazed components.

Acknowledgements

The authors would like to thank Jim Coleman, Nat Saenz, and Shelly Carlson for their assistance in metallographic and SEM sample preparation and analysis. This work was supported by the US Department of Energy, Office of Fossil Energy, Advanced Research and Technology Development Program. The Pacific Northwest National Laboratory is operated by Battelle Memorial Institute for the United States Department of Energy under Contract DE-AC06-76RLO 1830.

References

- [1] de Biasi V. *Gas Turbine World* 2003;33:12.
- [2] Kovacic G, Oguztoreli M, Chambers A, Ozum B. *Inter. J. Hydr. Energy* 1990;15:125.
- [3] Dyer PN, Richards RE, Russek SL. *Proceedings of the sixth international symposium on solid oxide fuel cells (SOFC VI)* 1999;1:1173.
- [4] Steele BCH. *Mater. Sci. Eng. B* 1992;13:79.
- [5] Payne R, Chen SL, Wolsky AM, Richter WF. *Comb. Sci. Tech.* 1989; 67:1.
- [6] Abrardo JM, Bennett DL, Carolan MF, Chen CM, Schinski WL, Steppan JJ, Waldron WE. *Proceedings of the 2004 AIChE spring national meeting* 2004; 1:1406.
- [7] Kothari R, Buddhi D, Sawhney RL. *Inter J. Global Energy Iss.* 2004; 21:154.
- [8] Armor AF, Preston GT. *Energy Conv. Manag.* 1996;37:671.
- [9] Lobachyov K, Richter HJ. *Trans ASME J. Energy Res. Tech.* 1996; 118:285.
- [10] Kivisaari T, Bjornbom P, Sylwan C, Jacquinot B, Jansen D, de Groot A. *Chem. Eng. J.* 2004;100:167.
- [11] Kharton VV, Yaremchenko AA, Naumovich EN, Marques FMBJ. *Sol. St. Electrochem.* 2000;4:243.
- [12] Slade RCT, Singh N. *Sol. St. Ionics* 1991; 46:111.
- [13] Stambouli AB, Traversa E. *Renew. Sust. Energy Rev.* 2002;6:433.
- [14] Simner SP, Stevenson JWJ. *Pow. Sources* 2001;102:310.
- [15] U.S. Department of Energy SECA website: www.doe.gov/seca.
- [16] Yang Z, Xia G, Meinhardt KD, Weil KS, Stevenson JWJ. *Mater. Eng. Perf.* 2004;13:327.
- [17] Yang Z, Stevenson JW, Meinhardt KD. *Sol. St. Ionics* 2003; 160:213.
- [18] Weil KS, Deibler JE, Hardy JS, Kim DS, Xia GG, Chick LA, Coyle CAJ. *Mater. Eng. Perf.* 2004;13:316.
- [19] Nicholas MG, Peteves SD. *Scr. Met. Mater.* 1994;31:1091.
- [20] Rice JP, M.S. Thesis 2004; Washington State University.
- [21] Weil KS, Coyle CA, Hardy JS, Kim JY, Xia GG. *Fuel Cell Bull.* 2004; 2004:1.
- [22] Erskine KM, Meier AM, Pilgrim SM. *J. Mater. Sci.* 2002;37:1705.
- [23] Hardy JS, Kim JY, Weil KSJ. *Electrochem. Soc.* 2004;151:J43.
- [24] Roth RS, Dennis JR, McMurdie HF, eds. *Phase diagrams for ceramists*, Volume VI 1987; The American Ceramic Society.
- [25] Simner SP, Bonnett JF, Canfield NL, Meinhardt KD, Shelton JP, Sprenkle VL, Stevenson JWJ. *Pow. Sources* 2003;113:1.
- [26] Weil KS, Kim JY, Hardy JS. *Electrochem. Sol. St. Lett.* 2005;8:A133.
- [27] Loehman RE, Tomsia APJ. *Am. Cer. Soc.* 1994;77:271.
- [28] Kofstad P. *High temperature corrosion* 1988; Elsevier Applied Science Publishers.
- [29] Nishiura H, Suzuki RO, Ono K, Gauckler LJ. *J. Amer. Ceram. Soc.* 1998; 81:2181.
- [30] Grugel RN, Hellowell A. *Met. Trans. A* 1981;12:669.
- [31] Kim JY, Hardy JS, Weil KS. *J. Electrochem. Soc.* 2005;152:J52.
- [32] Mukerjee S, Shaffer S, Zizelman J, Chick L, Baskaran S, Coyle C, Chou Y-S, Deibler J, Maupin G, Meinhardt K, Paxton D, Peters T, Sprenkle V, Weil S. *Proceedings of the eighth international symposium on solid oxide fuel cells (SOFC VIII)* 2003;1:736.